Properties of samples containing natural gas hydrate from the JAPEX/JNOC/GSC Mallik 2L-38 gas hydrate research well, determined using Gas Hydrate And Sediment Test Laboratory Instrument (GHASTLI)

W.J. Winters[1], I.A. Pecher[2], J.S. Booth[1], D.H. Mason[1], M.K. Relle[1], and W.P. Dillon[1]

Winters, W.J., Pecher, I.A., Booth, J.S., Mason, D.H., Relle, M.K., and Dillon, W.P., 1999: Properties of samples containing natural gas hydrate from the JAPEX/JNOC/GSC Mallik 2L-38 gas hydrate research well, determined using Gas Hydrate And Sediment Test Laboratory Instrument (GHASTLI); in *Scientific Results from JAPEX/JNOC/GSC Mallik 2L-38 Gas Hydrate Research Well, Mackenzie Delta, Northwest Territories, Canada, (ed.) S.R. Dallimore, T. Uchida, and T.S. Collett; Geological Survey of Canada, Bulletin 544, p. 241–250.*

Abstract: As part of an ongoing laboratory study, preliminary acoustic, strength, and hydraulic conductivity results are presented from a suite of tests conducted on four natural-gas-hydrate-containing samples from the Mackenzie Delta JAPEX/JNOC/GSC Mallik 2L-38 gas hydrate research well. The gas hydrate samples were preserved in pressure vessels during transport from the Northwest Territories to Woods Hole, Massachusetts, where multistep tests were performed using GHASTLI (Gas Hydrate And Sediment Test Laboratory Instrument), which recreates pressure and temperature conditions that are stable for gas hydrate. Properties and changes in sediment behaviour were measured before, during, and after controlled gas hydrate dissociation. Significant amounts of gas hydrate occupied the sample pores and substantially increased acoustic velocity and shear strength.

Résumé : Les résultats préliminaires de tests acoustiques, de résistance et de conductivité hydraulique effectués sur quatre échantillons contenant des hydrates de gaz naturels prélevés dans le puits de recherche sur les hydrates de gaz JAPEX/JNOC/GSC Mallik 2L-38, dans le delta du Mackenzie, sont présentés dans le cadre d'une étude en laboratoire actuellement en cours. Les échantillons d'hydrates de gaz ont été transportés, dans des récipients sous pression, des Territoires du Nord-Ouest jusqu'à Woods Hole, au Massachusetts, où ils ont été soumis à des essais à multiples étapes à l'aide d'un instrument de laboratoire destiné à l'exécution de tests sur les hydrates de gaz et les sédiments qui a recréé les conditions de pression et de température dans lesquelles les hydrates de gaz sont stables. Les propriétés des sédiments et les changements de leur comportement ont été mesurés avant et après la dissociation contrôlée des hydrates de gaz et au cours de cette dissociation. Un important volume d'hydrates de gaz occupait les interstices des échantillons, ce qui a considérablement augmenté la vitesse acoustique et la résistance au cisaillement.

[1] United States Geological Survey, Center for Coastal and Marine Geology, 384 Woods Hole Road, Woods Hole, Massachusetts 02543, U.S.A.
[2] Institute for Geophysics, University of Texas, Austin, Texas 78759, U.S.A.

INTRODUCTION

Recently, there has been a renewed interest by domestic and international organizations in the study of natural gas hydrate as a potential new energy resource and as a geohazard. Gas hydrate is a crystalline solid composed of water and natural gas that is stable at high-pressure, low-temperature conditions found along many continental margins and also beneath permafrost in Arctic regions (Kvenvolden et al., 1993; Booth et al., 1996). Determination of the properties of gas hydrate is greatly complicated by its instability upon removal from in situ pressure and temperature conditions. With logistical co-operation from the Geological Survey of Canada (GSC), we have preserved the natural-gas-hydrate-containing samples obtained from the outer Mackenzie Delta and have re-established in situ conditions on individual test samples using GHASTLI. Acoustic velocity, amount of gas hydrate in the pore space, shear strength, and hydraulic conductivity were measured before, during, and after controlled gas hydrate dissociation.

Four natural-gas-hydrate-bearing samples (Test no. GH058, GH059, GH060, and GH062) recovered from the Mallik 2L-38 gas hydrate research well, located at lat. 69°27′40.71″N, long. 134°39′30.37″W, between the depths of 898 and 913 m (RKB — relative to the kelly bushing on the drill rig which is 8.31 m above sea level; Collett et al., 1999) were studied in this program . Two other samples depressurized, resulting in gas hydrate dissociation, during transport and two additional samples remain to be tested. The 1150 m deep well was drilled during February and March 1998, adjacent to the Beaufort Sea in the Mackenzie Delta, Northwest Territories, in a co-operative effort of the Japan Petroleum Exploration Company (JAPEX), the Japan National Oil Corporation (JNOC), the Geological Survey of Canada (GSC), the United States Geological Survey (USGS), and numerous other government organizations and private companies. Resistivity, sonic transit-time, gamma-ray, and other logging results from a nearby hydrocarbon exploratory well (Mallik 2L-38 drilled by Imperial Oil Ltd. in 1972; Bily and Dick, 1974) provided valuable insight about geologic conditions, including the location of gas hydrate layers.

In situ, sample pores contained a combination of gas hydrate and brackish water, but little or no free gas, and no ice, because the temperature at 900 m is about 7°C (Wright et al., 1999). However, in situ pore water was converted to ice during the recovery process as a result of endothermic cooling induced by gas hydrate dissociation (Dallimore et al., 1999a). Laboratory procedures were able to reverse the process and convert the ice to water while retaining the gas hydrate. Although the properties measured on the gas-hydrate- and water-containing samples are the most relevant to in situ conditions at Mallik 2L-38, the results for samples with ice present are included because of their potential similarity to gas-hydrate-bearing sediments thought to occur within the permafrost itself (Dallimore and Collett, 1995). Unintentional freezing of the samples may have produced a critical benefit by stabilizing the noncemented sand in a similar manner to that used on important geotechnical engineering projects that intentionally use ground freezing to obtain high-quality cores in sandy material.

GEOLOGICAL SETTING AND LOCATION OF GAS HYDRATE

In the Mackenzie Delta region, 11 transgressive-regressive stratigraphic sequences have been identified above the lower Cretaceous structural basement, based on well-log interpretations and seismic-reflection data (Dixon and Dietrich, 1988; Dixon et al., 1992). Three of those sequences, ranging from Pleistocene to Oligocene, exhibited unique gamma-ray well-log records, and were tentatively identified in the Mallik 2L-38 well (Dallimore et al., 1999a; Jenner et al., 1999). The Iperk Sequence (0–346 m) primarily consists of coarse sand with some conglomerate and organic-rich layers. The Mackenzie Bay Sequence (346–932 m) is also sandy, with a finer component near the Iperk Sequence and interbedded gravel layers lower in the sequence. It has been inferred that a dolomite-cemented sandstone layer separates the Mackenzie Bay Sequence from the Kugmallit Sequence (>932 m), the latter being composed of interbedded sand and silt with rare lignite beds (Jenner et al., 1999). The bottom of ice-bearing permafrost is located at approximately 640 m, based on the resistivity log (Collett, et al., 1999).

Natural gas hydrate was observed in the Mallik 2L-38 well typically as pore filling or as grain coatings within coarse-grained sand and gravel deposits between 897 and 922 m (Collett et al., 1999; Dallimore et al., 1999a; Winters et al., 1999). Nodules less than 1 cm in diameter and thin veins less than 1 mm thick were also observed. Well logs suggest that gas hydrate exists below the level of sample recovery to a depth of about 1110 m (Collett et al., 1999; Dallimore et al., 1999a). The ‘standard’ Archie relation used for interpretation of the electrical-resistivity logs indicates that hydrate occupies an average of 47% of the void space in situ (Collett et al., 1999), but gas-yield experiments from recovered samples in which gas hydrate was intentionally dissociated suggest that approximately 30% of the pore space was occupied at the time of dissociation. This is reasonable since the gas hydrate was outside its P-T stability zone for about 1 to 1.5 hours during recovery (Dallimore et al., 1999a). It is estimated that gas hydrate in the nearby Mallik L-38 well occupies an average of about 67% of the void space (Collett and Dallimore, 1998).

METHODS AND EQUIPMENT

Field

Two conventional Baker Hughes Inteq core barrels were used to recover 37 m of core with sample diameters of 133 mm and 89 mm between 886 m and 952 m (Dallimore et al., 1999a). Four sediment samples (each approximately 260 mm long) containing gas hydrate were saved for GHASTLI testing. The diameters of the first (collected from 899.10–899.36 m) and second (collected from 898.84–899.10 m) core samples were trimmed from 133 mm to about 70 mm in order to fit inside transportation pressure vessels (76 mm inside diameter and approximately 270 mm long). About 45 minutes were required to trim the first sample and an additional

30-45 minutes were needed for the second. At the end of that time, gas hydrate in subsamples from a nearby section of core still dissociated actively when immersed in a dish of water. Evidently, the gas hydrate was stabilized by the self-preservation phenomena described by Ershove and Yakushev (1992). The two remaining samples (collected from 902.96–903.22 m and 913.00–913.26 m) fit directly into pressure vessels without trimming. The 260 mm long samples were cut approximately in half with a hack saw before being stored in the pressure vessels.

The four transportation vessels, each containing two test samples, were pressurized with methane gas to about 9 MPa. Two specimens of the methane used for pressurization were preserved for isotopic analysis. The pressure vessels were stored at -6 to -10°C for the overland trip to Woods Hole, Massachusetts. During transport, the sample recovered from 902.96–903.22 m dissociated due to a tubing failure. The remaining six pressurized samples were maintained at -10°C until they were ready for testing.

GHASTLI

Overview

Gas Hydrate And Sediment Test Laboratory Instrument (GHASTLI) integrates a number of complex instrumentation systems designed to establish the pressure and temperature conditions necessary to induce gas hydrate formation within natural or reconstituted sediment, or to preserve naturally existing gas hydrate samples (Fig. 1, 2; Booth et al., 1994; Winters et al., 1994). A maximum pressure of 25 MPa can be applied to a 70 mm diameter by 130 mm test sample within a silicone-oil-filled main pressure vessel. Internal sediment pore pressure can be maintained at lower values relative to the external confining pressure to impart an isotropic consolidation stress, σ'_c, simulating in situ overburden pressure.

The test-sample perimeter is surrounded by flexible membranes, and top and bottom end caps incorporate acoustic transducers and gas- or water-flow ports. The bottom end cap rests on an interchangeable internal load cell. The top end cap is contacted by a variable-temperature bath-controlled heat exchanger which imparts a unidirectional cooling front downward through the specimen. To achieve better sample thermal equilibrium, the perimeter of the main pressure vessel is also surrounded by cooling coils.

Syringe pumps that are both flow-rate and pressure controllable are used to maintain the confining pressure surrounding the specimen, as well as the internal specimen pressures which include seawater pore pressure, methane gas pressure, and back pressure. The back pressure system contains a collector that is capable of separating and measuring water and gas volumes at test pressures that are pushed out of the specimen by the dissociation of gas hydrate. The syringe pump that controls the seawater pressure also moves the load ram during the shear phase. Electrical resistance measurements were recorded horizontally at eight discrete points along the perimeter; however, the data are still being analyzed and will not be presented at this time.

Acoustics

P-wave velocity is measured by transmission through the specimen using 1 MHz (natural frequency) wafer-shaped crystals that are located on the back side (away from the specimen) of each end cap. A pulser sends an electrical signal, with a 400 volt pulse height, to the transmitting transducer. The received signal typically has a 200 kHz frequency and is amplified, digitized, displayed on a digital oscilloscope, and recorded by a computer. Acoustic P-wave velocity, V_p, is calculated from the specimen length/measured traveltime corrected for system delays.

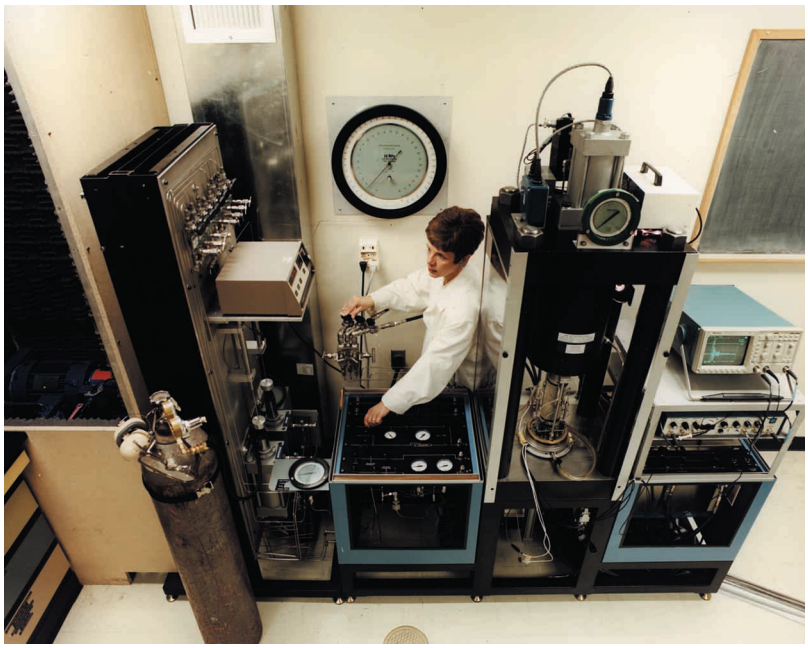

Figure 1.

Gas Hydrate And Sediment Test Laboratory Instrument (GHASTLI). Syringe pumps and computer systems are not visible. Photograph courtesy of W.J. Winters.

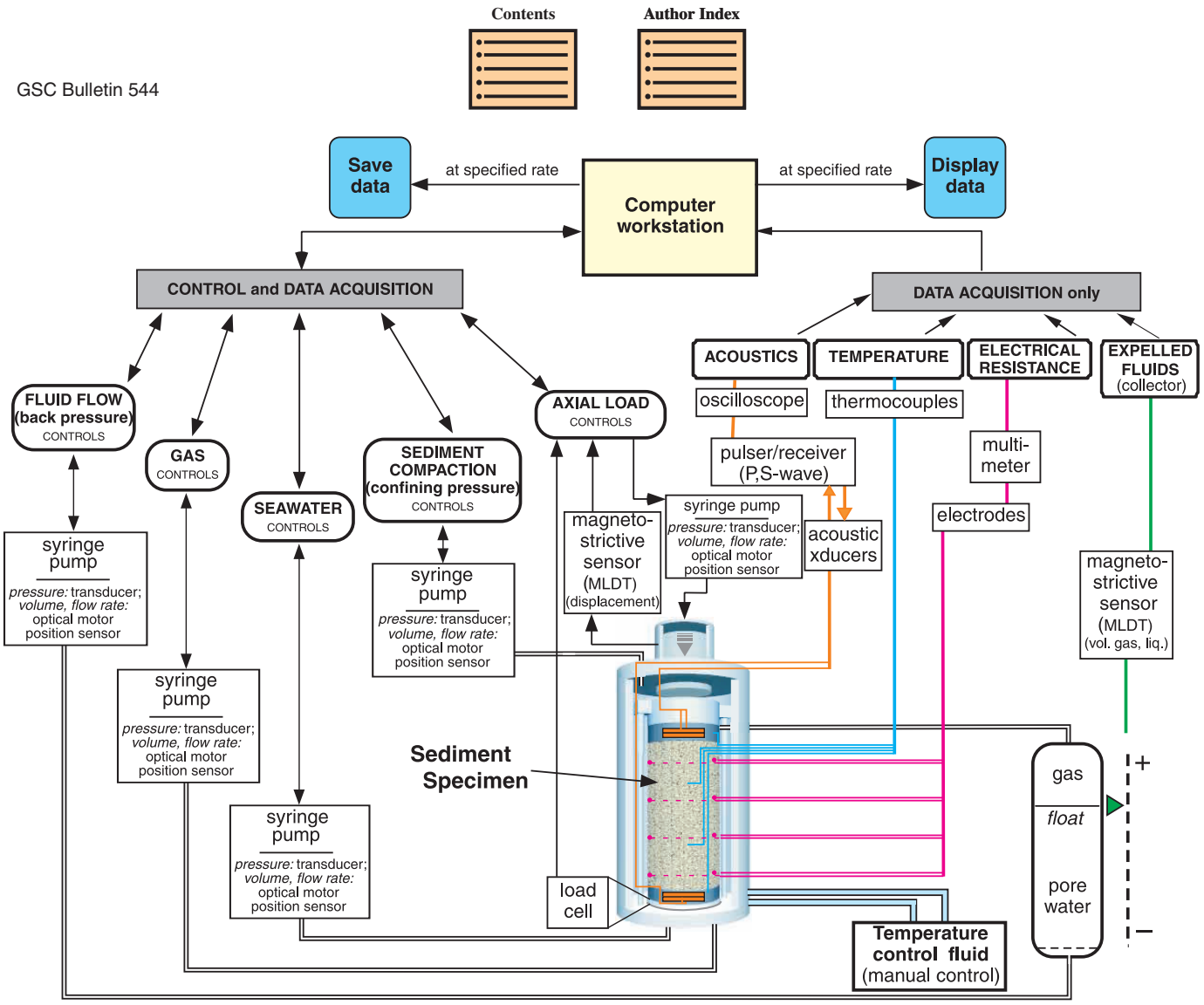

Figure 2. *Schematic of GHASTLI showing main pressure and data acquisition systems.*

Strength

Four parameters were measured during triaxial strength tests: load, axial deformation, confining pressure, and pore pressure. Loading is produced by a syringe-pump-controlled ram contacting the heat exchanger which then pushes on the sample at a rate related to the syringe pump piston travel. Movement of the ram, which can vary from 0.0001 mm/min to 2 mm/min, is measured using a linear-displacement transducer. Interchangeable load cells can be varied according to anticipated strength of the specimen.

Hydraulic conductivity

Hydraulic conductivity measurements were performed (according to procedures in American Society for Testing and Materials (1998), modified for use with syringe pumps) at different phases of testing by flowing seawater from the bottom end cap up through the specimen and out the top end cap into a back-pressure silicone oil/seawater interface chamber. Both constant flow rate and constant head methods were used. Pressure, flow rates, and fluid volume were recorded from the syringe pumps and the pressure drop through the specimen was measured with a variable-range differential-pressure transducer or by comparing pressure differences between syringe pumps.

Laboratory methods

GHASTLI

Because core pore waters were frozen upon recovery, the Mallik 2L-38 test samples were kept frozen prior to placement in GHASTLI. The presence of ice helped to stabilize the hydrate at atmospheric pressure during the test set-up procedures. Although the specimens were still partially frozen at the beginning of testing, they were allowed to thaw in order to measure properties with only gas hydrate (but not ice) present, to more accurately simulate in situ conditions.

Each of the four GHASTLI laboratory tests consisted of different steps designed to facilitate certain physical property measurements. Initially, the test specimen was removed from a pressurized transportation vessel within a walk-in freezer. The cylindrical specimen was jacketed and enclosed between two instrumented end caps before being brought to the lab.

The test sample was placed into GHASTLI and pressures (between 8 and 12 MPa) and temperatures (near 2°C) conducive to hydrate stability were quickly re-established. In situ hydrostatic pressure was estimated at approximately 9 MPa. An effective consolidation stress, σ'_c, was then imposed on the sample to partially recreate in situ overburden pressure. Because a σ'_c of 3 MPa caused the first sample (GH058) to perforate the enclosing membranes, a substantially lower pressure difference (0.25 MPa) was used for the three remaining tests. Acoustic measurements were performed at different consolidation stresses to ascertain the effect on acoustic velocity.

Initial acoustic measurements on the gas hydrate and partially ice-bonded sample were followed by converting the ice to water. Temperature was raised to approximately 4°C for at least 24 hours until all ice had melted and acoustic velocity stabilized.

After all of the ice (which was not present in situ) had melted, temperature was slowly raised in 1 to 2°C increments until dissociation began. The dissociated gas, specimen pore water, and water released from hydrate entered the back-pressure collector where water and gas were separated and their volumes measured. After gas generation had apparently ceased, temperature was raised an additional 2 to 4°C to insure that all hydrate had dissociated completely. A sample of the gas from the collector was preserved. A geochemical comparison of the gas from the collector to that used for pressurization during transport of the samples is currently being conducted to determine if additional gas hydrate formed from the methane used for pressurization.

In all cases, the P-wave signal previously established was lost during initial dissociation of gas hydrate in the test samples. Numerous different methods were tried to re-establish the transmitted P-wave signal, including slowly flushing water up through the specimen to push out any remaining gas, but none of those procedures were successful in producing a valid acoustic signal. The eventually successful method required that the specimen be removed from GHASTLI, refrozen, and new membranes applied with additional acoustic couplant applied between the end caps and test specimen. The refreezing stabilized the unconsolidated sandy specimen during the complete sample 'rebuilding' procedure. One strength test was performed on a sample (GH062) that contained gas hydrate; the rest were sheared after dissociation. Finally, the specimen was removed again from GHASTLI and the volume and wet and dry mass were measured for index-property calculations.

Texture

Specimen texture was determined by first drying the sample at 90°C for at least 24 hours to determine dry mass, washing through a 0.063 mm mesh sieve with a 0.4% solution of sodium hexametaphosphate to separate the coarse and fine fractions, and washing again with fresh water. Subsequently, the coarse sample was dry sieved and a pipette analysis was performed on the fine fraction.

RESULTS AND DISCUSSION

Index properties and gas hydrate quantity

Salinity-corrected water contents were determined for specimens dried at 90°C for at least 24 hours, using two different definitions (Table 1). The water-content calculations include all water in the sample, both free water and water that had been incorporated into gas hydrate. Porosity values were back-calculated from initial and final mass measurements assuming 100% pore-space saturation and adjusting for the volumetric expansion of water in gas hydrate. The two pairs of adjacent or nearly adjacent samples have relatively consistent mass physical properties. Measurements performed on adjacent smaller-sized specimens produced similar values (Winters et al., 1999; Dallimore et al., 1999b).

The quantities of gas hydrate present in the pore space at the beginning of tests GH059, GH060, and GH062, were determined from measurements of the initial porosities and the amounts of gas only recovered in the collector during gas hydrate dissociation. As such, the calculated gas hydrate quantities represent minimum values. The amount of methane present, in moles, was determined from the equation of state relationships presented by Duan et al. (1992).

Table 1. Depth intervals and initial mass physical properties of test samples. The amounts of gas hydrate contained in the sediment voids are estimated values and were calculated from the volume of gas measured in the collector after dissociation.

Test ID	GH058	GH059	GH060	GH062
Depth interval (m)	913.00–913.13	913.13–913.26	898.97–899.10	899.23–899.36
Salinity-adjacent (ppt)	12	12	4	4
Water content (M_w/M_s) (%)	21.3	20.6	15.5	17.9
Water content (M_w/M_t) (%)	17.5	17.1	13.4	15.1
Porosity (%)	37.2	36.5	30.0	33.0
Voids filled at 90% cage occupancy (%)	–	53	38	35
Voids filled at 80% cage occupancy (%)	–	55	40	37
Voids filled at 70% cage occupancy (%)	–	58	42	39

Notes: M_w = mass of water
M_s = mass of sediment solids
M_t = mass of total specimen

Table 2. Results of texture analyses.

	Sieve mesh opening		GH058	GH059	GH060	GH062
	(phi)	(mm)	(% retained)	(% retained)	(% retained)	(% retained)
Gravel	-3	8.0	2.61	3.38	0.00	0.00
	-2	4.0	0.00	0.00	0.00	0.00
	-1	2.0	0.57	0.19	0.00	0.00
Total			3.18	3.57	0.00	0.00
Sand	0	1.0	0.60	0.09	0.00	0.02
	1	0.5	7.46	6.62	2.58	2.07
	2	0.25	67.69	65.93	68.66	69.99
	3	0.125	14.25	16.21	15.49	16.66
	4	0.0625	3.07	3.83	5.16	4.18
Total			93.07	92.67	91.90	92.93
Silt	8	0.0039	2.53	2.49	6.93	5.64
Clay			1.22	1.27	1.17	1.43

The proportion of sand present in each sample is nearly identical and varies from 92 to 93% (Table 2). Medium-grained sand is the predominant size fraction. The deeper samples (GH058 and GH059) contained about 3% gravel, while GH060 and GH062 had slightly greater amounts of silt.

Acoustic properties

P-wave signals were recorded (Figs. 3–5) and velocities, V_p, were calculated at numerous times during the tests (Table 3). Knowledge of the material occupying the pore space and the consolidation stress is critical to understanding the implications of the various velocity measurements. Most of the P-wave velocities reported are lower than those determined from well logging (Collett et al., 1999; Miyairi, et al., 1999) perhaps partly because of the smaller σ'_c values used in the laboratory to prevent the samples from puncturing the surrounding membranes. P-wave velocity values increased with consolidation stress in GH058 because of the greater grain-to-grain contact stress (primarily) and increased density, but the rate of velocity change decreased with increasing pressure (Fig. 6). Sample shortening during consolidation could also create an apparent velocity increase due to reduced travel distance for the acoustic pulse. However, because the specimen is predominantly sand, this is expected to be a minor factor. P-wave velocities similar to field values were obtained at the highest consolidation stresses. The decrease in velocity with increasing pressure for test GH062 may have been caused by melting of water ice within the specimen (Table 3).

The velocities obtained in the laboratory can be compared with theoretical field-velocity predictions of Lee et al. (1993) by using the nomograph presented by Miyairi et al. (1999) for sediment with known porosity. The expected amount of gas hydrate present in the GHASTLI samples can also be estimated from that nomograph. The predicted degree of pore filling by gas hydrate is 30% for GH058, 28% for GH059, 0% for GH060, and 10% for GH062, based on the test-specimen porosity and measured laboratory velocities. The discrepancy between measured and predicted hydrate quantity based on V_p values is again partly a result of the difference between field and laboratory effective consolidation stresses. The relation between laboratory acoustic velocity and estimated amount of sediment voids filled with gas hydrate is shown in Figure 7.

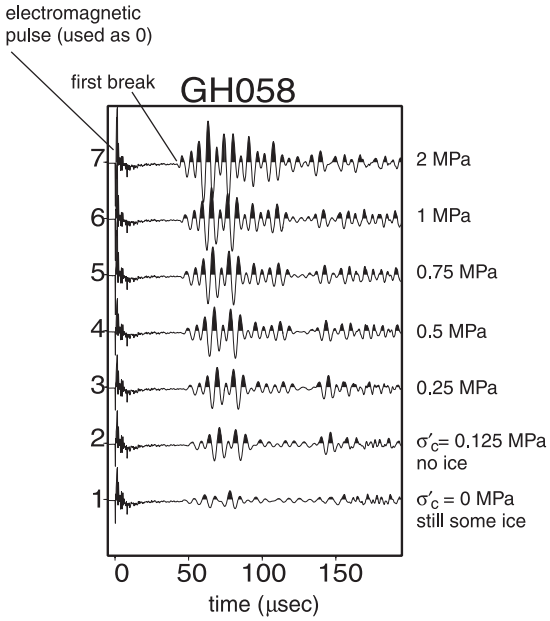

Figure 3. *Compressional-wave signals from test no. GH058 indicating the influence of consolidation stress (σ'_c) on velocity and signal strength. An earlier first arrival represents a faster P-wave velocity. Signal amplitudes show relative trends, but are not to scale.*

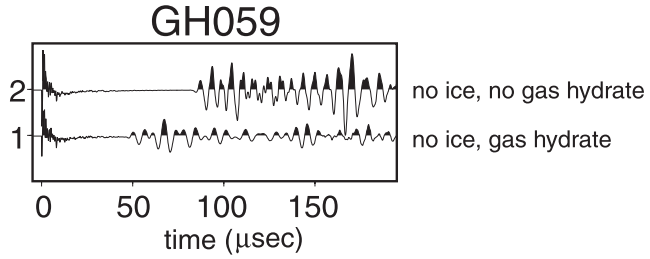

Figure 4. *Compressional-wave signals from test no. GH059 indicating that velocity decreased after gas hydrate dissociated. An earlier first arrival represents a faster P-wave velocity. Signal amplitudes show relative trends, but are not to scale.*

There are some clear trends in the velocity data (Table 3). For example, during test GH058, an 18% increase in V_p was measured with an effective stress increase from 0 to 2 MPa, and a 35% decrease was calculated after ice melted and gas hydrate dissociated with σ'_c equal to 0.125 MPa. Decreases in V_p of 47%, 26%, and 25% were observed after gas hydrate dissociation in tests GH059, GH060, and GH062, respectively. However, sample GH059 contained unfrozen water and may have also contained free gas after 'rebuilding', causing a lower V_p value. A 39% decrease in velocity was calculated for the gas-hydrate-containing GH060 specimen after the ice melted, but only a 7% decrease was observed for GH062 under similar conditions.

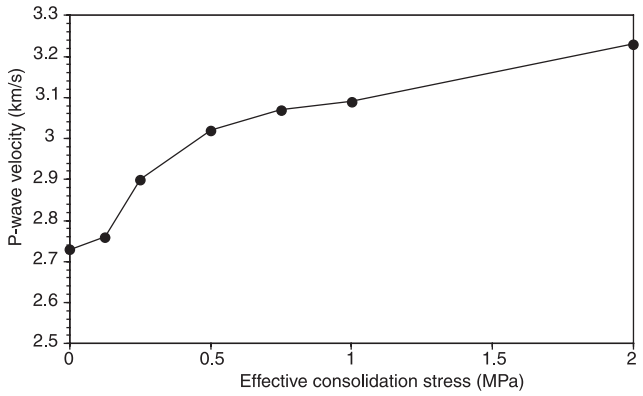

Figure 6. *Effective consolidation stress, σ'_c, versus the P-wave velocity for test no. GH058. Results do not account for specimen shortening caused by consolidation.*

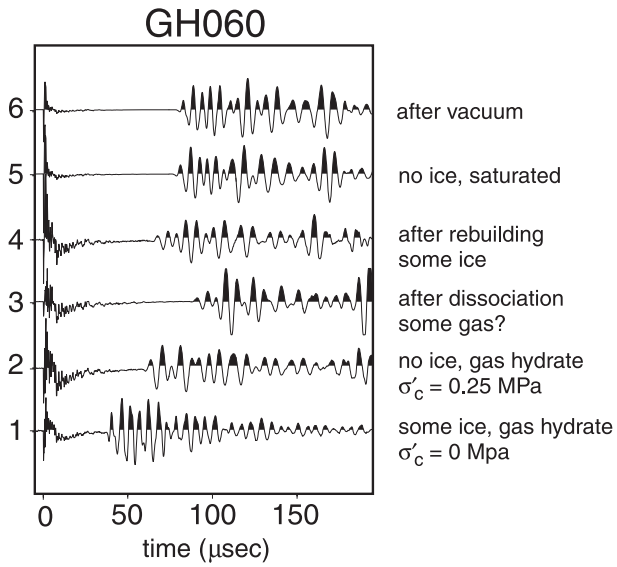

Figure 5. *Compressional-wave signals from test no. GH060 indicating that the presence of ice and gas hydrate increased velocity. An earlier first arrival represents a faster P-wave velocity. Signal amplitudes show relative trends, but are not to scale.*

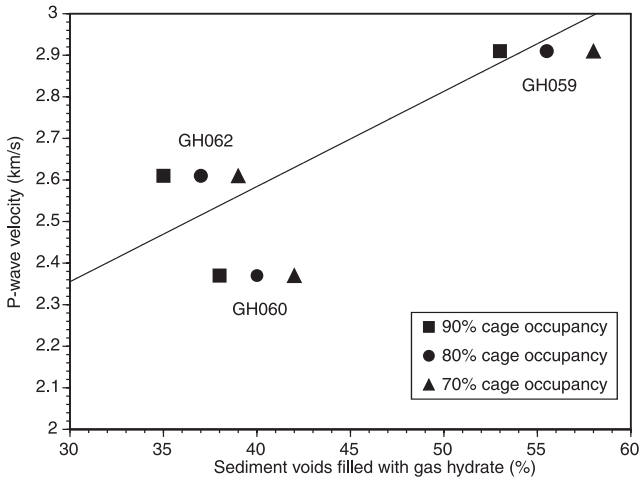

Figure 7. *Acoustic P-wave velocity related to the estimated amount of sediment void space filled by gas hydrate as determined from the quantity of dissociated gas in the collector.*

Table 3. Compressional-wave velocities for specimens with varying pore-space contents at different effective consolidation stresses, σ'_c.

Pore-space contents				Vp (km/s)			
Partially frozen	Gas hydrate	Unfrozen water	σ'_c (MPa)	GH058	GH059	GH060	GH062
●	●		0	2.73		3.88	2.80
●	●		0.125	2.76			2.66
●	●		0.25	2.90			2.65
●	●		0.50	3.02			
●	●		0.75	3.07			
●	●		1.0	3.09			
●	●		2.0	3.23			
	●		0.25		2.91	2.37	2.61
●			0			2.14a	3.48a,b
?		●	0.125	1.80a			
		●	0.25		1.54a,c	1.55c 1.77a 1.73a	1.97a,b

a: test specimen was removed from GHASTLI in order to restore acoustic coupling
b: after shear phase
c: may contain gas

The cause of P-wave signal loss during initial hydrate dissociation is unknown. However, attenuation due to the presence of free gas appears to be responsible for some of the loss.

Strength properties

If gas hydrate behaves similarly to ice in sediment, then the gas-hydrate-bonded material should, in most cases, be stronger than comparable sediment that does not contain gas-hydrate-bonded material. Andersland and Anderson (1978) stated that the presence of ice can increase the strength of sediment to that of weak concrete. Frozen sediment exhibits a wide range in strength properties because strength is influenced by a number of factors: strain rate, temperature, confining pressure, grain size, and density. The strength of sediment containing gas hydrate is probably influenced by these and other factors such as gas hydrate cage occupancy.

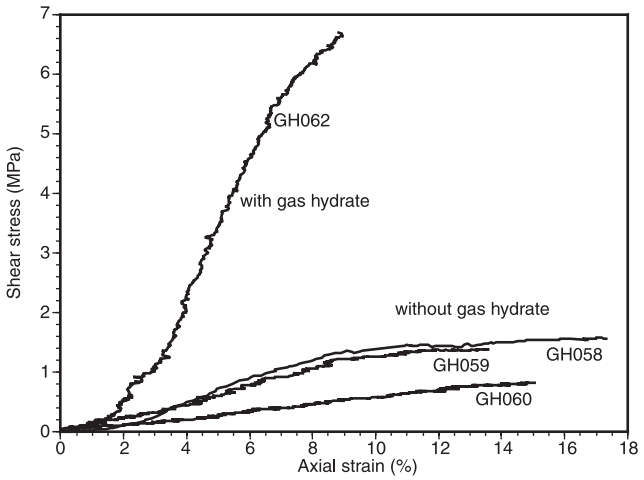

Figure 8. *Triaxial shear stress plotted as a function of axial strain for specimens with and without gas hydrate.*

Undrained triaxial shear tests were performed on each of the test specimens. Samples GH058 through GH060 were sheared after the gas hydrate was dissociated, whereas GH062 was sheared while hydrate, but not ice, was still present within the specimen. Plots of the shear stress vs. axial strain for the four test samples show that the strength of the sample containing gas hydrate is indeed much higher (Fig. 8). The gas-hydrate-containing sample exhibited high negative pore pressures during shear. Andersland and Ladanyi (1994) indicated that frozen samples are typically plotted with respect to total stresses because of the difficulty in measuring intergranular stresses. Evidently, the Mallik 2L-38 specimen pores contained enough free water to transmit pore pressures.

Interesting trends are apparent from the triaxial test data (Table 4). Although GH060 and GH062 were nearly adjacent to each other and therefore are most appropriate for comparison, all tests were compared for completeness. In all categories, the gas-hydrate-containing sample (GH062) was strongest: maximum shear strength (q_{max}) of the hydrate sample was 4.3 to 8.1 times stronger; q_{max} normalized for consolidation stress was 2.9 to 5.8 times stronger; and deviator stress was 4.3 to 8.1 times stronger than the non-hydrate samples. However, the amount of strain imparted to the four samples varied. GH062 was stopped at 8.8% strain because of the very high negative pore pressures built up that could have potentially caused the test specimen to perforate the surrounding membranes. If the other test parameters are calculated at 8.8% strain, the following comparisons are apparent: the q_{max} for the hydrate sample is 5.1 to 12.8 times stronger; and the q_{max} normalized for consolidation stress is 3.4 to 9.3 times stronger than other non-hydrate samples. The shear strength

Table 4. Triaxial strength test results.

Test ID	GH058	GH059	GH060	GH062
Depth interval (m)	913.00–913.13	913.13–913.26	898.97–899.10	899.23–899.36
Pore contents	water	water	water	gas hydrate
Initial water content (M_w/M_s) (%)	21.3	20.6	15.5	17.9
Consolidation stress, σ'_c (MPa)	0.24	0.22	0.26	0.36
'A' coefficient at failure	-0.33	-0.31	-0.26	-0.26
q at failure (q_{max}) (MPa)	1.55	1.38	0.82	6.69
p' at failure (MPa)	2.80	2.45	1.53	10.54
q_{max}/σ'_c	6.5	6.2	3.2	18.6
Deviator stress at failure (MPa)	3.09	2.76	1.65	13.38
Axial strain at failure (%)	15.0	13.4	15.0	8.8
ϕ'_{max} (degrees)	37.5	38.6	33.8	44.4
q at 8.8% axial strain (MPa)	1.32	1.22	0.52	6.69
q at 8.8% axial strain/σ'_c	5.5	5.5	2.01	18.6

Notes:
GH058, GH059, GH060 were sheared after gas hydrate dissociation, refreezing, rejacketing, and re-consolidation procedures
GH062 was stopped at 8.8% axial strain to prevent membrane rupture due to high negative pore pressures
'A' coefficient at failure = change in pore pressure/change in deviator stress
q = shear stress acting on a plane inclined at 45° from the horizontal, $(\sigma_1 - \sigma_3)/2$
p' = normal effective stress acting on a plane inclined at 45° from the horizontal, $(\sigma'_1 + \sigma'_3)/2$
ϕ'_{max} = maximum friction angle in terms of effective stresses, passes through the origin

Table 5. Hydraulic conductivity test results.

Test	Rebuilding		Frozen		Gas hydrate			Hydraulic conductivity (x10^{-7} cm/s)			
								Constant pressure		Constant flow	
GH	Pre-	Post-	Partly	Non-	Yes	No	Comments	DPT	SyPump	DPT	SyPump
058		●		●		●		22	6	7	5
059	●			●		●		29	23	51	35
060	●			●		●		206	124	227	104
060		●		●		●		401	334	214	129
060		●		●		●	some fines removed	1200	491	813	215
062	●		●		●			–	962?	–	598?
062	●			●	●			147a	133a	111a	96a
062		●	●			●		343a	297a	335a	311a
062		●		●		●		635a	392a	502a	264a

Notes: DPT: Differential pressure transducer
SyP: Syringe pump pressure difference
a: after shear phase

measured for the gas-hydrate-bearing sample is within, but on the low side, of the wide range encountered for frozen sands (Andersland and Ladanyi, 1994).

Although the magnitude of negative pore pressure was very high in GH062, it was proportionally the same or of lower magnitude than the other tested samples. The A coefficient (change in pore pressure during shear/change in deviator stress) values of -0.26 to -0.33 are indicative of dense fine sand (Hunt, 1984). Because the A coefficient changes with density, for example, it would be approximately +2.0 to +3.0 for a very loose sand, it is believed that the test sample densities are similar. That is, the refreezing procedure used after dissociation during tests GH058, GH059, and GH060, did not greatly influence the density. The maximum effective friction angle, ø′, for the hydrate sample was also the highest value of any of the tests. The friction angles for the non-gas-hydrate-bearing samples are within the typical range of sandy sediment (Hunt, 1984).

Depending upon the amount present, gas hydrate has the potential to greatly affect the mechanical properties of the host sediment.

Hydraulic conductivity

Hydraulic conductivity values can vary over a wide range and depend on a number of sediment parameters, including grain size, porosity, structure, discontinuities, and tortuosity; and fluid parameters such as viscosity (Cedergren, 1977; Holtz and Kovacs, 1981). Sometimes, a small amount of fine-grained sediment or a small change in water content can greatly influence permeability. Hydraulic conductivity measurements were performed on sediment that contained different materials in the pores at various times during testing (Table 5). The change in pore filling resulted from methods used to melt ice in the sediment voids while preserving gas hydrate and procedures to re-establish acoustic signals after hydrate dissociation. The hydraulic conductivity values are low to very low, and on average, correspond to those of a medium sand or silty sand (Lambe and Whitman, 1969; Cedergren, 1977), but considerable scatter is present in the test data.

Adjacent test samples GH058 and GH059 have lower hydraulic conductivities than the other samples although they have higher initial porosities. Typically, the ‘rebuilding’ process (used to re-establish acoustic signals and which included refreezing the sample) increased the permeability. However, the opposite occurred in tests GH058 and GH059 if we assume that the specimens had similar initial permeabilities. Melting of pore ice present in GH062 after rebuilding appears to have increased the hydraulic conductivity, as did the removal of some fine-grained sediment during vacuum saturation at the end of GH060. The most unexpected result was the anomalously high hydraulic conductivity exhibited in the initial test on sample GH062 (containing both ice and gas hydrate). This may have been due to the presence of natural or testing-induced fractures, or to the difficulty of performing permeability tests on specimens that contain different phase mixtures without affecting the sample itself (M.B. Clennell, pers. comm., 1999). The pressure drop across the differential-pressure transducer was so low at times that those values were discarded. Because these results cannot be readily explained, they should be viewed as tentative until testing on the remaining adjacent gas hydrate samples has been completed.

Changes in texture, density, and pore filling influenced hydraulic conductivity of the specimens tested in this study. Hydraulic conductivity in the vertical direction probably changes significantly at Mallik 2L-38 because stratigraphy and porosity change within the gas-hydrate-bearing zone. This variation in permeability may have contributed to the in situ non-uniform distribution of gas hydrate with depth.

CONCLUSIONS

Sand samples containing natural gas hydrate were recovered from the Mallik 2L-38 well and stored at pressures and temperatures that promoted gas hydrate stability. Acoustic, triaxial strength, and hydraulic conductivity measurements were performed at different stages of testing using GHASTLI. Properties of the test specimens changed significantly as the contents of sediment pores varied. P-wave velocity of specimens containing gas hydrate decreased at least 25% after dissociation. Undrained triaxial shear strength was 3 to 9 times greater for a sample containing gas hydrate compared to similar

specimens without hydrate. Such changes in behaviour, including strength loss if dissociation occurs, must be considered during drilling operations in gas-hydrate-bearing zones, not only in the Arctic but offshore on continental margins as well.

ACKNOWLEDGMENTS

J.F. Wright and R. Oldale provided helpful reviews. S.R. Dallimore, T.S. Collett, F.M. Nixon, J.F. Wright, and T. Uchida provided assistance with sample recovery at the drill site, logistics, and/or post-recovery transportation of the samples. A. Robinson and L. Poppe provided textural results from the test samples. The drillers and staff at the drill site are thanked for their assistance with core recovery. Any use of trade names is for descriptive purposes only and does not imply endorsement by the USGS.

REFERENCES

Andersland, O.B. and Anderson, D.M.
1978: Geotechnical engineering for cold regions; McGraw-Hill Book Company, New York, New York, 566 p.

Andersland, O.B. and Ladanyi, B.
1994: An introduction to frozen ground engineering; Chapman & Hall, New York, 352 p.

American Society for Testing and Materials
1998: Standard test method for permeability of granular soils (constant head) D 2434-68 ; *in* American Society for Testing and Materials, Annual Book of ASTM Standards, West Conshohocken, Pennsylvania, p. 202–206.

Bily, C. and Dick, J.W.L.
1974: Naturally occurring gas hydrates in the Mackenzie Delta, N.W.T.; Bulletin of Canadian Petroleum Geology, v. 22, no. 3, p. 340–352.

Booth, J.S., Rowe, M.M., and Fischer, K.M.
1996: Offshore gas hydrate sample database with an overview and preliminary analysis; United States Geological Survey, Open File Report 96-272, 23 p.

Booth, J.S., Winters, W.J., and Mason, D.H.
1994: Capabilities of GHASTLI for geo-gas hydrate research; United States Geological Survey, Open File Report 94-646, 13 p.

Cedergren, H.R.
1977: Seepage, drainage, and flownets; John Wiley & Sons, New York, New York, 534 p.

Collett, T.S. and Dallimore, S.R.
1998: Quantitative assessment of gas hydrates in the Mallik L-38 well, Mackenzie Delta, N.W.T., Canada; *in* Proceedings of the 7th International Conference on Permafrost, Yellowknife, Canada, Collection Nordicana, Université Laval, p. 189–194.

Collett, T.S., Lewis, R., Dallimore, S.R., Lee, M.W., Mroz, T.H., and Uchida, T.
1999: Detailed evaluation of gas hydrate reservoir properties using JAPEX/JNOC/GSC Mallik 2L-38 gas hydrate research well downhole well-log displays; *in* Scientific Results from JAPEX/JNOC/GSC Mallik 2L-38 Gas Hydrate Research Well, Mackenzie Delta, Northwest Territories, Canada, (ed.) S.R. Dallimore, T. Uchida, and T.S. Collett; Geological Survey of Canada, Bulletin 544.

Dallimore, S.R. and Collett, T.S.
1995: Intrapermafrost gas hydrates from a deep core hole in the Mackenzie Delta, Northwest Territories, Canada; Geology, v. 23, no. 6, p. 527–530.

Dallimore, S.R., Collett, T.S., and Uchida, T.
1999a: Overview of science program, JAPEX/JNOC/GSC Mallik 2L-38 gas hydrate research well; *in* Scientific Results from JAPEX/JNOC/GSC Mallik 2L-38 Gas Hydrate Research Well, Mackenzie Delta, Northwest Territories, Canada, (ed.) S.R. Dallimore, T. Uchida, and T.S. Collett; Geological Survey of Canada, Bulletin 544.

Dallimore, S.R., Laframboise, R.R., Fotiou, M., and Medioli, B.E. (comp.)
1999b: JAPEX/JNOC/GSC Mallik 2L-38 gas hydrate research well, Mackenzie Delta, Northwest Territories, Canada: interactive data viewer; Geological Survey of Canada, Open File D3726, 1 CD-ROM.

Dixon, J. and Dietrich, J.R.
1988: The nature of depositional and seismic sequence boundaries in Cretaceous–Tertiary strata of the Beaufort–Mackenzie Basin; *in* Sequences, Stratigraphy, Sedimentology: Surface and Subsurface, (ed.) D.P. James and D.A. Leckie; Canadian Society of Petroleum Geologists, Memoir 15, p. 63–72.

Dixon, J., Dietrich, J.R., and McNeil, D.H.
1992: Upper Cretaceous to Pleistocene sequence stratigraphy of the Beaufort–Mackenzie and Banks Island areas, northwest Canada; Geological Survey of Canada, Bulletin 407, 90 p.

Duan, Z., Moller, N., and Weare, J.H.
1992: An equation of state for the CH_4-CO_2-H_2O system: I. pure systems from 0 to 1000°C and 0 to 8000 bar; Geochimica et Cosmochimica Acta, v. 56, p. 2605–2617.

Ershove, E.D. and Yakushev, V.S.
1992: Experimental research on gas hydrate decomposition in frozen rocks; Cold Regions Science and Technology, v. 20, p. 147–156.

Holtz, R.D. and Kovacs, W.D.
1981: An introduction to geotechnical engineering; Prentice-Hall, Inc., Englewood Cliffs, New Jersey, 733 p.

Hunt, R.E.
1984: Geotechnical Engineering Investigation Manual; McGraw-Hill Book Company, New York, 983 p.

Jenner, K.A., Dallimore, S.R., Clark, I.D., Paré, D., and Medioli, B.E.
1999: Sedimentology of gas hydrate host strata from the JAPEX/JNOC/GSC Mallik 2L-38 gas hydrate research well; *in* Scientific Results from JAPEX/JNOC/GSC Mallik 2L-38 Gas Hydrate Research Well, Mackenzie Delta, Northwest Territories, Canada, (ed.) S.R. Dallimore, T. Uchida, and T.S. Collett; Geological Survey of Canada, Bulletin 544.

Kvenvolden, K.A., Ginsburg, G.D., and Soloviev, V.A.
1993: Worldwide distribution of subaquatic gas hydrates; Geo-Marine Letters, v. 13, p. 32–40.

Lambe, T.W. and Whitman, R.V.
1969: Soil mechanics; John Wiley & Sons, New York, New York, 553 p.

Lee, M.W., Hutchinson, D.R., Dillon, W.P., Miller, J.J. Agena, W.F., and Swift, B.A.
1993: Method of estimating gas hydrates in deep marine sediments; Marine and Petroleum Geology, v. 10, p. 493–506.

Miyairi, M., Akihisa, K., Uchida, T., Collett, T.S., and Dallimore, S.R.
1999: Well-log interpretation of gas-hydrate-bearing formations in the Mallik 2L-38 gas hydrate research well; *in* Scientific Results from JAPEX/JNOC/GSC Mallik 2L-38 Gas Hydrate Research Well, Mackenzie Delta, Northwest Territories, Canada, (ed.) S.R. Dallimore, T. Uchida, and T.S. Collett; Geological Survey of Canada, Bulletin 544.

Winters, W.J., Booth, J.S., Nielsen, R.R., Dillon, W.P., and Commeau, R.F.
1994: A computer-controlled gas hydrate-sediment formation and triaxial test system; *in* International Conference on Natural Gas Hydrates, (ed.) E.D. Sloan, Jr., J. Happel, and M.A. Hnatow; Annals of the New York Academy of Sciences, v. 715, New York, New York, p. 490–491.

Winters, W.J., Dallimore, S.R., Collett, T.S., Katsube, J.T., Jenner, K.A., Cranston, R.E., Wright, J.F., Nixon, F.M.,and Uchida, T.
1999: Physical properties of sediments from the JAPEX/JNOC/GSC Mallik 2L-38 gas hydrate research well; *in* Scientific Results from JAPEX/JNOC/GSC Mallik 2L-38 Gas Hydrate Research Well, Mackenzie Delta, Northwest Territories, Canada, (ed.) S.R. Dallimore, T. Uchida, and T.S. Collett; Geological Survey of Canada, Bulletin 544.

Wright, J.F., Dallimore, S.R., and Nixon, F.M.
1999: Influences of grain size and salinity on pressure-temperature thresholds for methane hydrate stability in JAPEX/JNOC/GSC Mallik 2L-38 gas hydrate research well sediments; *in* Scientific Results from JAPEX/JNOC/GSC Mallik 2L-38 Gas Hydrate Research Well, Mackenzie Delta, Northwest Territories, Canada, (ed.) S.R. Dallimore, T. Uchida, and T.S. Collett; Geological Survey of Canada, Bulletin 544.